ACS APPLIED ELECTRONIC MATERIALS

Article

Self-cleaning and self-powered UV sensor for highly reliable outdoor UV detection

Qi Xu, Junjie Lou, Ruichao Zhang, Binbin Ma, Suo Bai, and Yong Qin

ACS Appl. Electron. Mater., **Just Accepted Manuscript** • DOI: 10.1021/acsaelm.0c00215 • Publication Date (Web): 10 May 2020

Self-cleaning and self-powered UV sensor for highly reliable outdoor UV detection

Qi Xu[a], *Junjie Lou*[b], *Ruichao Zhang*[b], *Binbin Ma*[b], *Suo Bai*[b] *and Yong Qin*[b]*

[a] School of Advanced Materials and Nanotechnology, Xidian University, Xi'an 710071, China

[b] Institute of Nanoscience and Nanotechnology, Lanzhou University, Lanzhou 730000, China

KEYWORDS: UV sensor, ZnO, nanogenerator, self-cleaning, self-powered nanodevice

ABSTRACT: Improving the individual node's reliability and long-time working ability are important for the giant wireless sensor networks. In this paper, a kind of self-cleaning and self-powered UV sensor (SSUS) with the ability to give the intensity value of UV light and against the dust contamination was developed. To avoid the influence of dust, the SSUS can realize a self-cleaning function by either wind/water. This character makes the SSUS be a good UV sensor in real environment especially in dust environment with high reliability. In addition, after the SSUS is calibrated by a few parameters, it can give the UV intensity according to the SSUS's output directly with a deviation about 3% in a self-powered manner, even the output of SSUS is not linearly dependent on UV intensity.

INTRODUCTION

UV sensors have important applications in many areas such as water quality testing, mineral inspection, ultraviolet communication, and flame detection.[1-3] Wireless Sensor Network (WSN)[4] which born from the joint of sensor technology, microelectric technology, wireless communication technology and embedded technology, can greatly improve the UV sensors' ability in acquiring information in above areas. The bottle neck that restricts the development of WSN is the long power supply of individual node in the WSN.[5] Traditionally, the power of the individual node is supplied by batteries. However, with the expansion of network scale and the increase of the number of nodes, monitoring and replacing the depleted batteries is a great challenge.

Replacing power supplies from traditionally batteries with new power source which can convert the ambient energy into electricity is a promising way to solve the above challenge.[4] Among these new power sources, piezoelectric nanogenerators (PENGs)[6-7] are very competitive. On one hand, compared with solar energy and thermal energy, the mechanical energy is undoubtedly a kind of energy that is not limited by time and region. On the other hand, compared with triboelectric nanogenerators (TENGs)[8] which are also widely used to harvest the ambient mechanical energy[9-11] and UV sensing,[12] the PENGs possess high mechanical endurance and durability[13] without the risk of material abrasion. With the increase of the output of the PENGs,[14-19] it has the more feasibility to be used to power the UV sensors. Xu showed a self-powered UV sensor constructed by a PENG and a ZnO nanowire-based UV sensor connected in series, where the voltage drop across the sensor can be used to detect the UV light.[20] Later, the self-powered UV sensors develop toward three directions. One direction towards improving the PENG's output to make the self-powered UV sensor's signal detection independent of high precision measurement or additional energy storage unit, such as using large amount of aligned nanofibers with high piezoelectric coefficient to improve the PENG's integration degree,[21] adopting single crystal ferroelectric nanowire,[22] utilizing the Maxwell–Wagner–Sillars (MWS) polarization in composite piezoelectric material.[23] Another direction towards developing wearable self-powered UV sensor for real time personal health protection, such as weaving individual piezoelectric active materials to form a two dimensional textile structure,[24] improving single piezoelectric fiber's robustness,[25] developing electronic skin.[26-27] The final research direction towards forming a compact structure, in which power unit and the sensing unit is the same one, such as via the collective oscillation of embed metal particles under UV light in the composite PENG to control the piezoelectric material's polarization state and thereby to control the PENG's output.[28]

Albeit the rapid development of self-powered UV sensors, in order to make a further step toward practical application of the self-powered UV sensors, there are two points needed to be noticed. First, there doesn't exist linear relationship between the UV intensity and the self-powered sensor's output. Although we have a few fixed UV intensity points, how to determine the intensity of the UV light according to the output of the self-powered UV sensors outside the tested points is unsolved. Second, as for the

WSN containing many nodes, its practical working condition is usually in outdoor environment and full of dust. The gradual degradation of the transmittance caused by the accumulation of surrounding dust will decrease the penetrated light arrived on the sensors,[29] and thus make a large difficulty for accurately measure the UV intensity. So, maintaining the node's cleanness is critically important.

Here, we developed a self-cleaning and self-powered UV sensor (SSUS) which can be used to reliably detect the UV intensities according to its output voltage in dust environment. By applying a superhydrophobic coating, the accumulated dust on the sensor can be cleaned easily by water or wind, and the voltage signal is only 0.3%/2.8% larger than that of the original signal, which shows the sensor's outstanding self-cleaning ability. After the fitting parameters are determined according to the tested points, the intensities (0.040 and 0.60 mW/cm^2) of the UV light can be determined with a deviation about 3%, even there doesn't exist linear relationship between the UV intensity and the SSUS's output.

RESULTS AND DISCUSSION

The structure of SSUS is schematically illustrated in **Figure 1**a, where a self-cleaning UV sensor is in serial connected with a PENG and the output of the SSUS is the voltage drop across the self-cleaning UV sensor. The PENG was fabricated by dispersing $BaTiO_3$ nanoparticles (**Figure S1**a) into the PDMS matrix with a mass ratio of 40%. The nanoparticles are in tetragonal structure (Figure S1b) with lattice parameters *a* and *c* equal to 4.02 Å and 4.04 Å, respectively. The piezoelectric coefficient d_{33} of $BaTiO_3$ nanoparticles is 118 pC/N. In practice, the $BaTiO_3$ nanoparticles are not spherical and periodically arranged in the composite film as the schematic shows. Nevertheless, the $BaTiO_3$ nanoparticles are dispersed evenly into the matrix (Figure 1b), and this will contribute to the improvement of the PENG's output.[30] The thickness of the PDMS/BaTiO3 is about 40 μm. In order to increase the output change of SSUS toward the intensity variation of UV light, an ultrathin hexagonal ZnO film as shown in Figure 1c was used for fabricating UV sensor, as pointed by our previous work[31] this structure is superior for improving UV sensor's response. In order to improve the sensor's stability against moisture[32], a thin layer epoxy was used to package the UV sensor.

The performance of the PENG and UV sensor was characterized, respectively. By periodically bending and releasing the PENG via a linear motor, the PENG with an area of 15 cm^2 shows a maximum peak output voltage of 0.25 V as shown in **Figure 2**a. During the switching-polarity test in which the positive and negative probes of the voltage meter are connected to the negative and positive ends of the PENG, respectively, the output signal is reversed as shown in Figure 2b, and this confirmed that the signal is the real signal not an artifact.[7] Figure 2c shows the typical I-V curves of the sensor in dark and under UV illumination with intensity of 0.30 mW/cm^2 and wavelength of 365 nm. The I-V curves in dark and UV illumination are both linear, which indicates the carbon electrode forms an Ohmic contact with the ZnO film. Under an UV intensity of 0.30 mW/cm^2, the current reached a value of 10.4 nA at 1 V bias voltage, in contrast to the dark current of 23.7 pA. The dynamic behavior of the UV sensor was characterized from the time-resolved photocurrent measurements by alternatively exposing the sensor to UV light and dark as shown in Figure 2d. The sensor's rise and decay time, which are the time required for the current to increase to 90% of the steady-state photocurrent value and to decrease again by 90%, were also characterized. The rise and decay time were 15.2 s and 10.6 s, respectively.

The dynamic behavior of the SSUS was characterized by alternatively exposing the sensor to UV light of 0.30 mW/cm^2 and dark as shown in **Figure 3**. In general, either voltage signal or current signal can be used for UV detection. However, as the impedance type of PENGs is capacitive[33], the PENGs usually have a large voltage but low current. In addition, the UV sensor's resistance is also large (42.2 GΩ in dark environment, derived from Figure 1c), the current in the circuit will be reduced further. So, the voltage signal is chosen for UV detection and we didn't study the current change of the SSUS with the intensity of UV light. In the test period, the performance of the SSUS is stable. As the output of the SSUS is the voltage drop across the self-cleaning UV sensor, its value is sensitive to the resistance of the UV sensor. Upon illuminated by the UV light, along with the desorption of oxygen molecules from the ZnO film's surface, the resistance of the UV sensor decreased, and the output of the SSUS gradually changed from 0.23 V to 0.13 V. After turning off the UV light, along with the gradually adsorption of oxygen molecules on the ZnO surface, the resistance of the UV sensor increased, and the output of the SSUS gradually changed from 0.13 V to 0.23 V. The rise and decay time were 8.4 s and 10.9 s, respectively. Theoretically, the UV light can excite photogenerated carriers in $BaTiO_3$, which will increase of conductance of $BaTiO_3$ and lead to a reduced impedance of the PENTG. However, the density of photogenerated carriers n is related to the carrier lifetime τ,

$$n = \int \tau dG \tag{1}$$

where, τ is the carrier lifetime, G is the carrier generation rate, which is equal to the volume density of absorbed photons.[34] The lifetime of photogenerated carriers in $BaTiO_3$ are too short (in < 60 ps)[35] to generate appreciable generate appreciable carrier density changes in $BaTiO_3$. So, in practice, the influence of the UV on the PENG's impedance is negligible.

To solve the gradual degradation of the transmittance caused by the accumulation of surrounding dust, a superhydrophobic film with a contact angle of 155° (**Figure S2**) was used. The superhydrophobic coating is not an ordinary optically actively layer. The superhydrophobic coating can keep the UV sensor clean, as the accumulated dust on the sensor can be cleaned easily by water, especially by weak wind as schematically shown in **Figure 4**a, which means our sensor can keep clean even in an environment without water.   The detailed structure of the superhydrophobic surface is shown in Figure 4b. The surface of the superhydrophobic film is rough and full of uniformly distributed hump composed of cone shaped structures. The cone shaped structures with narrow tips and humps construct the superhydrophobic film's hierarchical structure. Packaged with this special film, the self-powered UV sensor (**Figure S3**a) simultaneously has the self-cleaning property. Under dark environment, as the UV sensor is packaged, so the dust will not affect the resistance of the UV sensor, and the output of the SSUS is not affected by the dust as shown in Figure 4c. Under UV illumination with intensity of 0.30 mW/cm^2, the dust will either shield or scatter the UV light, so the output of the SSUS will be affected by the dust as shown in Figure 4d. Upon sprinkling dust on the UV sensor (Figure S3b), due to the reduced penetrated UV light, the output of the SSUS changes from the initial value of 0.130 V to 0.189 V, which increases 45.4%. The reason is that the reduced penetrated will cause the resistance of the UV sensor larger than that of the original clean state. After the dust was cleaned by the wind generated by periodically squeezing a 5 mL plastic (Figure S3c), the output of the SSUS decreased to 0.139 V, which is 6.2% larger than that of the clean state. When the dust is further cleaned by the water (Figure S3d), the output of the SSUS decreased to 0.135 V, which is 3.9% larger than that of the clean state. These results show the SSUS has a good anti-dust property. This character makes the SSUS be a good UV sensor in real environment especially in dust environment with high reliability.

Finally, the self-powered UV sensor's output under different UV intensities was tested as shown in **Figure 5**a. As the UV intensity increases, the output of the SSUS decreased in a nonlinear way. There does not exist a simple way to relate these data. In order to obtain the value of the UV intensity from the output of SSUS outside the tested data, the relationship between these tested data is needed. To do this, analysis based on the equivalent circuit as shown in the inset of Figure 5a was conducted. The PENG is considered as a voltage source V generated by the piezoelectric potential and a capacitor

C of the PENG connected in serials,[36] and the UV sensor is considered as a photoresistor $G(P)$, where G is the conductance of the photoresistor, P is the intensity of the UV light. The output of the PENG can be approximated with a high accuracy as[37]

$$V = d*f/C \quad (2)$$

, where d is the piezoelectric constant of the PENG, f is the force exerted on the PENG. As for circuit analysis, the output of PENG is simplified as a sinusoidal voltage source. As only the frequency corresponding to the external driving frequency dominates, so using the sinusoidal voltage source for circuit analysis is effective. From the equivalent circuit, we can see that the voltage drop across the UV sensor is:

$$V(P) = \frac{df}{C}\frac{1}{\sqrt{1+\frac{G(P)^2}{\omega^2 C^2}}} \quad (3)$$

, where ω is the angular frequency of the external force. According to equation (3), in order relate V with P, the relationship between G and P is needed. The I-V characteristics of the UV sensor under UV light with different intensities is tested as shown in Figure 5b. The obtained conductance of UV sensor under different UV intensities is shown in Figure 5c. Their relationship obeys the power law $G(P)=G_0P^n$, which is caused by the complex process of electron-hole generation, trapping, and recombination within the semiconductor.[36] Combing with the equations of (2) and (3), a fitting equation as follows can be used to relate V with P.

$$V(P)=\frac{A}{\sqrt{1+BP^{n}}} \tag{4}$$

, where *A*, *B* and *n* are constant fitting parameters. To make the fitting more reliable, the number of input data should be greater than the parameters. The output of the SSUS under 0, 0.07, 0.30 and 1.10 mW/cm^2 were used to confirm the fitting curve and the obtained curve is

$$V(P)=\frac{0.24}{\sqrt{1+7.83P^{0.92}}} \tag{5}$$

In order to determine the UV intensity *P* according to the output of the SSUS *V*, the inverse function of equation (4) is obtained

$$P=\left(\frac{\left(\frac{0.244}{V}\right)^{2}-1}{7.827}\right)^{1.09} \tag{6}$$

The sensitivity of the SSUS *S* can be defined as,

$$S=\frac{\left|V_{\mathrm{UV}}-V_{\mathrm{dark}}\right|}{V_{\mathrm{dark}}}\times 100\% \tag{7}$$

where, V_{dark} and V_{UV} are of the output of SSUS under darkness and UV illumination, respectively. Under 0.07, 0.3 and 1.1 mW/cm^2 UV illumination, the sensitivity of the SSUS are 23.11%, 46.85% and 67.92%, respectively (Figure 5d). To test the accuracy of this curve, the points tested on the UV intensities of 0.04 and 0.60 mW/cm^2 was used. Under these intensities, the tested voltage is 0.205 and 0.102 V, respectively.

Substituting these values into equation (6), the obtained UV intensities are 0.04, and 0.58 mW/cm^2, and the deviation are 2.5%, and 3.3%, respectively.

CONCLUSION

In summary, a self-cleaning and self-powered UV sensor (SSUS) composed of PENG and a UV sensor was developed. When contaminated by dust, the SSUS can be cleaned by either wind/water, and after the cleaning process, the output of the SSUS has a deviation about 6.2%/ 3.9%, which shows a good self-cleaning ability. After analyzing the equivalent circuit of the SSUS and the conductance of the UV sensor versus the intensity of UV light, a fitting curve was given to predict the intensity of UV light according to the output of the SSUS. When the fitting parameters are determined, the intensities (0.040 and 0.60 mW/cm^2) of the UV light can be determined with a deviation about 3%, even there doesn't exist linear relationship between the UV intensity and the SSUS's output.

EXPERIMENTAL SECTION

Preparation of the PENG

Firstly, the polydimethylsiloxane (PDMS; Dow Corning Corp.) solution was prepared by adding curing agent into the base with a weight ratio of 1:10. Then, the $BaTiO_3$ nanoparticles (Aladdin, 99.99%, <100 nm) was dispersed into the PDMS with a mass ratio of 40% by ultrasonic wave. Then, the mixture was placed into the in vacuum condition (5 Pa) for 10 min. After the removal of air bubbles those were formed during ultrasonic wave, the mixture was spin coated onto an Cr/Ag electrode (3×5 cm) with a spinning rate of 3000 rpm for 30 s and then cured at 80 °C for 30 min to solidify the mixture. Next, the upper Cr/Ag electrode was sputtered. Interconnections were made using copper wires and carbon paste. Then the device was poled under an electric filed about 10 V/μm on the 120 ℃ hot plate for 2h.

To characterize the piezoelectric coefficient of $BaTiO_3$ nanoparticles, they are milled and pressed into a $BaTiO_3$ plate with a relatively high density under 220 MPa pressure, then sintered at 1200 ℃ for 3 h. The coefficient d_{33} is characterized on Quasi Static Piezoelectric D33 Meter (ZJ-6A).

Preparation of the self-cleaning UV sensors

Firstly, 0.15 M ammine-hydroxo zinc precursor solution was spun onto the cleaned glass substrate at 1000 rpm for 30 s, followed by a thermal annealing at 150 ºC for 2 h in air; then, carbon interdigital electrode with electrode spacing of 500 μm was screen printed on the ZnO film to form a UV sensor,[31] followed by the epoxy resin encapsulation. Finally, a superhydrophobic PDMS coating fabricated by a two-step reactive ion etching process[38] was covered on the UV sensor to form the final self-cleaning UV sensor.

The XRD pattern of ZnO was obtained from a film fabricated by drop coating method, where consecutive drops of the solution were deposited on the substate followed by thermal annealing at 150 ºC for 2 h in air, as the ZnO film fabricated by spin coating method was too thin to hardly obtain detectable signals.

Test method

The dark current and photoresponse of the self-cleaning UV sensor were performed using DS345 30 MHz synthesized function generator and SR 570 low-noise current preamplifier (**Figure S4**a). The DS345 30 MHz Synthesized Function Generator are capable of producing various patterns (sin, square, triangle, ramp) of voltage at a variety of frequencies (1 μHz to 30.2 MHz) and amplitudes (0.01 V to 10 V). The UV light intensity was quantified by a UV detector (Photoelectric Instrument Factory of Beijing Normal University, UV-A). The voltage from the self-cleaning and self-powered UV sensor under repeated bending and releasing driven by a LinMot linear motor (E1100) was measured (Figure S4b) by SR560 low-noise voltage preamplifier.

FIGURES

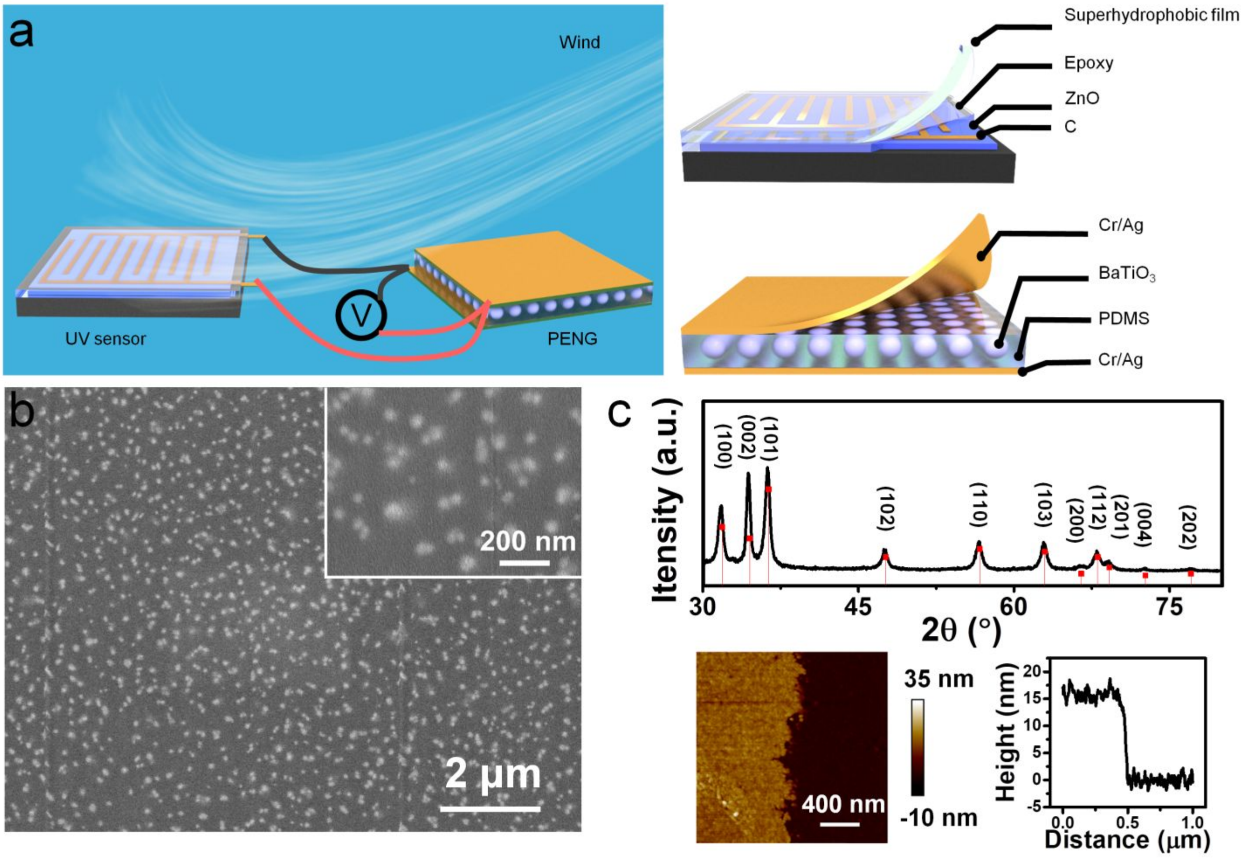

Figure 1. (a) The schematic of the self-cleaning and self-powered UV sensor. (b) SEM images of the $BaTiO_3$/PDMS composite film. (c) XRD and AFM images of the ZnO film.

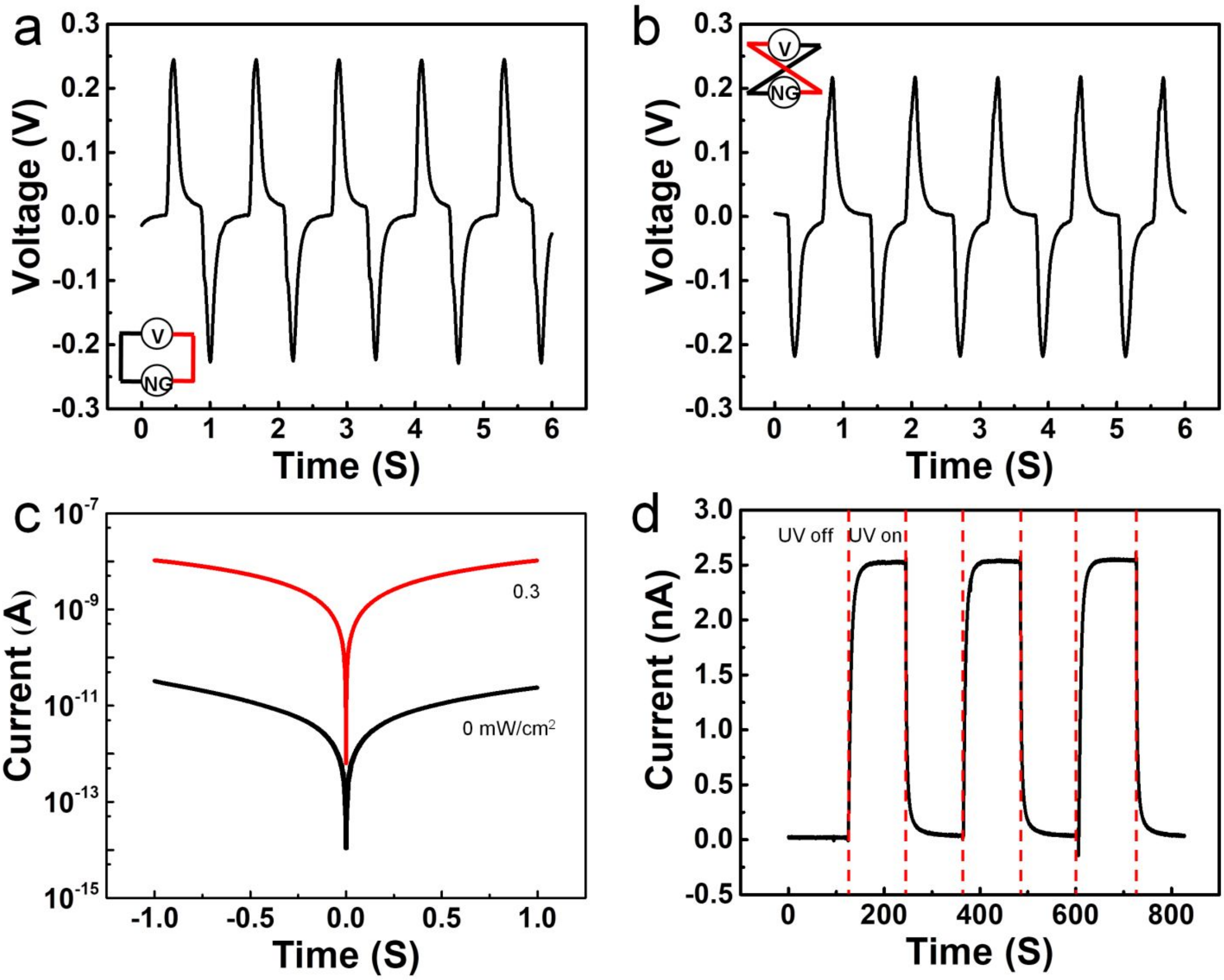

Figure 2. The output voltage of the piezoelectric nanogenerator under forward connection (a) and reversed connections (b), respectively. (c) The I-V characteristics of the UV sensor under dark and 365 nm UV light with intensity of 0.30 mW/cm^2, respectively. (d) The UV response of the UV sensor illuminated by the UV light with intensity of 0.30 mW/cm^2.

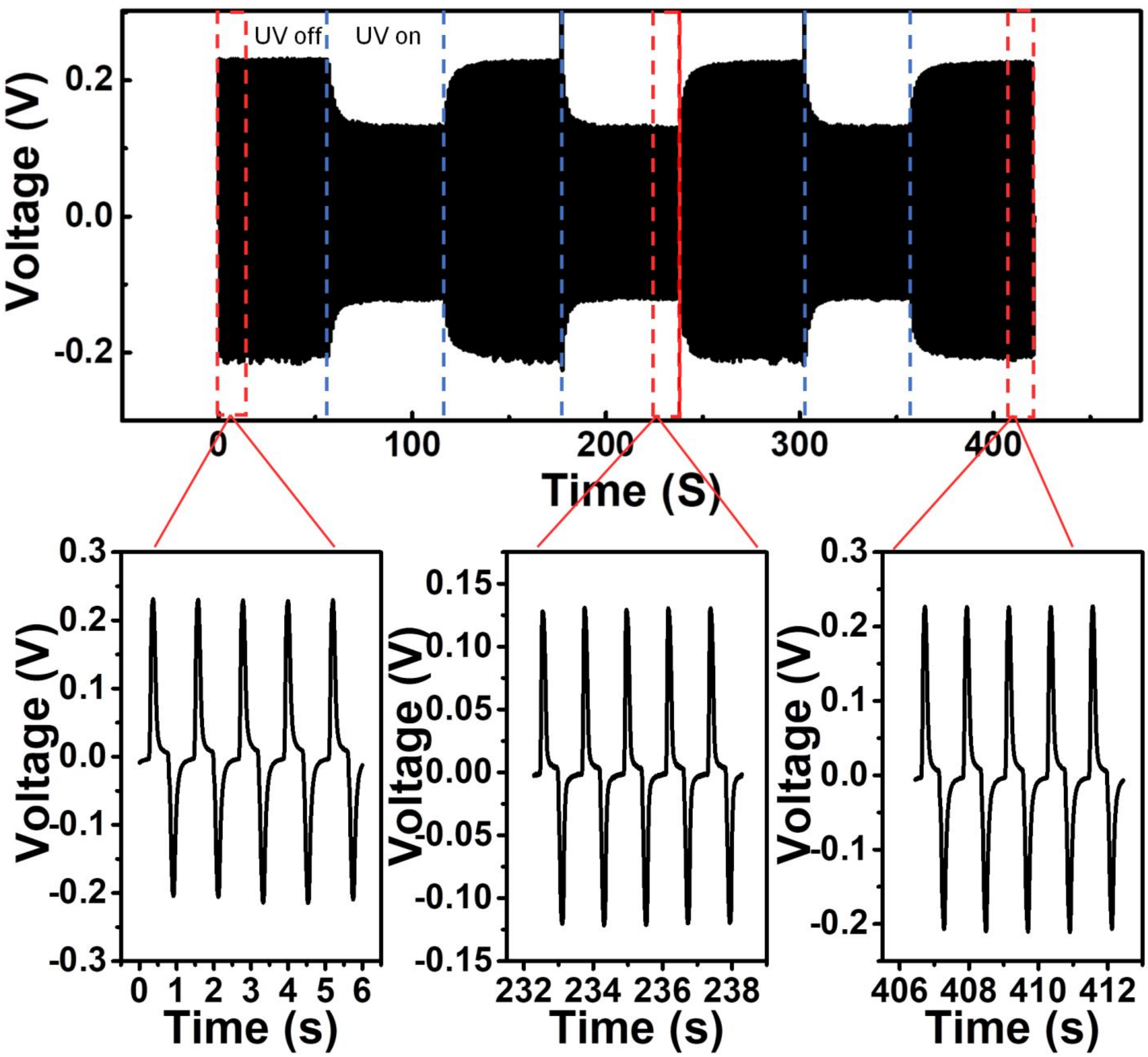

Figure 3. The UV response of the self-cleaning and self-powered UV sensor illuminated by the UV light with intensity of 0.30 mW/cm^2.

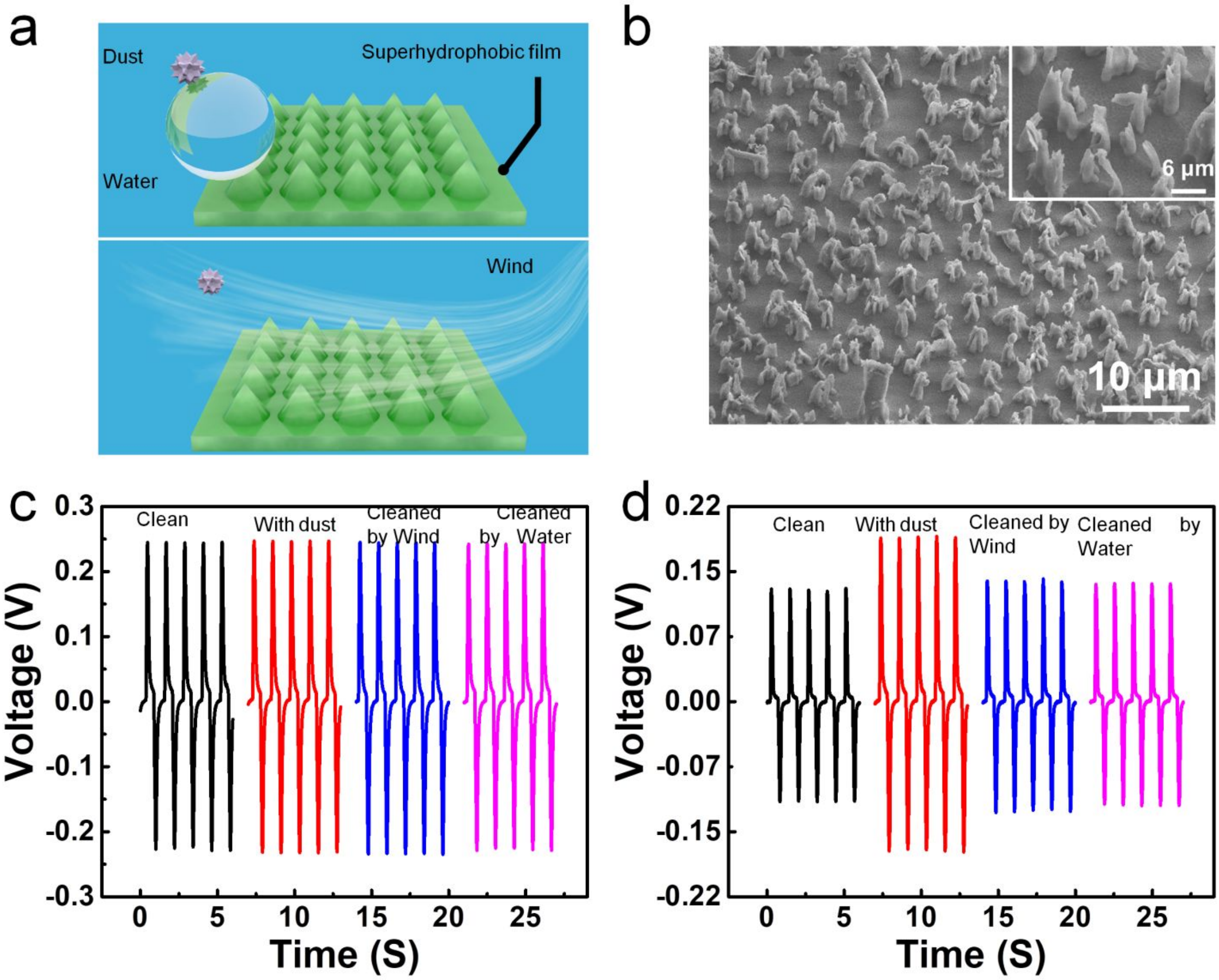

Figure 4. (a) The schematic of the self-cleaning process via the wind and the water. (b) SEM images of the superhydrophobic film. (c) Under dark state, the output of the self-cleaning and self-powered UV sensor when the sensor is clean, contaminated by dust, cleaned by wind, cleaned by water, respectively. (d) Under the UV light with intensity of 0.30 mW/cm^2, the output of the self-cleaning and self-powered UV sensor when the sensor is clean, contaminated by dust, cleaned by wind, cleaned by water, respectively.

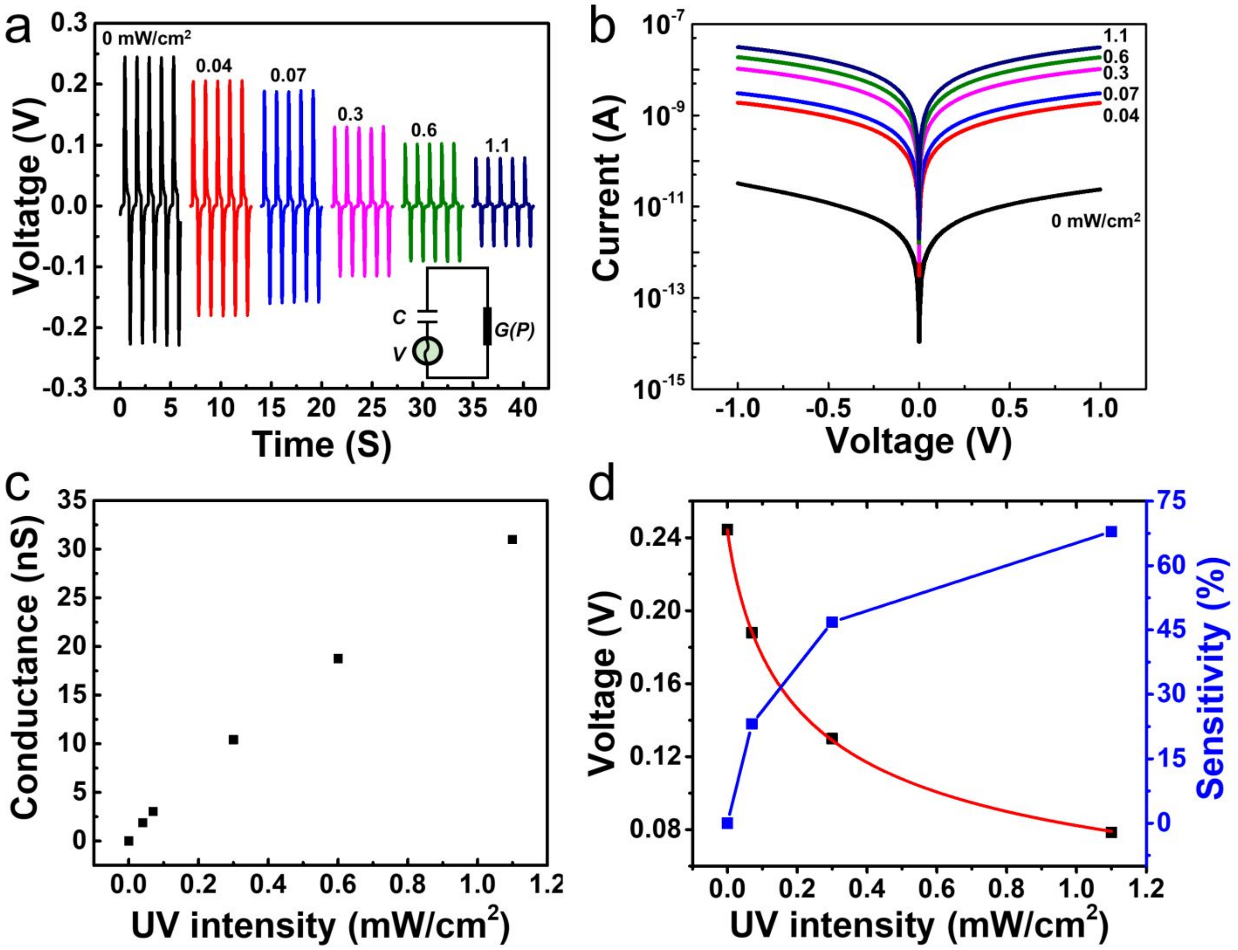

Figure 5. (a) The output of the self-cleaning and self-powered UV sensor under different UV intensities ranging from 0 to 1.10 mW/cm^2, respectively. The insert is the equivalent circuit of the self-cleaning and self-powered UV sensor. The I-V characteristics (b) and the deduced conductance (c) of the UV sensor under different UV intensities ranging from 0 to 1.10 mW/cm^2, respectively. (d) The relationship between the peak of the output of the self-cleaning and self-powered UV sensor under different UV intensities. The squares represent experimental data; the red curve is the fitted curve.

AUTHOR INFORMATION

Corresponding Author

E-mail: qinyong@lzu.edu.cn

Author Contributions

The manuscript was written through contributions of all authors. All authors have given approval to the final version of the manuscript.

ACKNOWLEDGMENT

We sincerely acknowledge the support from Joint fund of Equipment pre-Research and Ministry of Education (No. 6141A02022518), the National Program for Support of Top-notch Young Professionals, and the Fundamental Research Funds for the Central Universities (No. lzujbky-2018-ot04), NSFC (No. 81702095), The Project Supported by Natural Science Basic Research Plan in Shaanxi Province of China (2019JQ-652).

SUPPORTING INFORMATION

The Supporting Information is available free of charge via the Internet at http://pubs.acs.org/.

Figures about the SEM image, XRD spectrum (Figure S1); Photographs of a water droplet on the superhyndrophobic surface (Figure S2); Optical images of SSUS (Figure S3); Schematics about the measurements (Figure S4).

REFERENCES

(1) Monroy, E.; Calle, F.; Pau, J. L.; Munoz, E.; Omnes, F.; Beaumont, B.; Gibart, P. AlGaN-based UV photodetectors. *J. Cryst. Growth* **2001,** *230* (3-4), 537-543.

(2) Yu, A. G. Semiconductor near-ultraviolet photoelectronics. *Semicond. Sci. Technol.* **1999,** *14* (7), R41.

(3) Razeghi, M.; Rogalski, A. Semiconductor ultraviolet detectors. *J. Appl. Phys.* **1996,** *79* (10), 7433-7473.

(4) Akyildiz, I. F.; Kasimoglu, I. H. Wireless sensor and actuators networks: research challenges. *Ad Hoc Networks* **2004,** *2* (4), 351-367.

(5) Watral, Z.; Michalski, A. Selected problems of power sources for wireless sensors networks [instrumentation notes]. *IEEE Instrum. Meas. Mag.* **2013,** *16* (1), 37-43.

(6) Wang, Z. L.; Song, J. H. Piezoelectric nanogenerators based on zinc oxide nanowire arrays. *Science* **2006,** *312* (5771), 242-246.

(7) Yang, R. S.; Qin, Y.; Li, C.; Dai, L. M.; Wang, Z. L. Characteristics of output voltage and current of integrated nanogenerators. *Appl. Phys. Lett.* **2009,** *94* (2), 022905.

(8) Fan, F. R.; Tian, Z. Q.; Wang, Z. L. Flexible triboelectric generator! *Nano Energy* **2012,** *1* (2), 328-334.

(9) Zhu, G.; Zhou, Y. S.; Bai, P.; Meng, X. S.; Jing, Q.; Chen, J.; Wang, Z. L. A Shape-Adaptive Thin-Film-Based Approach for 50% High-Efficiency Energy Generation Through Micro-Grating Sliding Electrification. *Adv. Mater.* **2014,** *26* (23), 3788-3796.

(10) Ahmed, A.; Saadatnia, Z.; Hassan, I.; Zi, Y.; Xi, Y.; He, X.; Zu, J.; Wang, Z. L. Self-Powered Wireless Sensor Node Enabled by a Duck-Shaped Triboelectric Nanogenerator for Harvesting Water Wave Energy. *Adv. Energy Mater.* **2017,** *7* (7), 1601705.

(11) Li, S.; Peng, W.; Wang, J.; Lin, L.; Zi, Y.; Zhang, G.; Wang, Z. L. All-Elastomer-Based Triboelectric Nanogenerator as a Keyboard Cover To Harvest Typing Energy. *ACS Nano* **2016,** *10* (8), 7973-7981.

(12) Dai, Y.; Fu, Y.; Zeng, H.; Xing, L.; Zhang, Y.; Zhan, Y.; Xue, X. A Self-Powered Brain-Linked Vision Electronic-Skin Based on Triboelectric-Photodetecing Pixel-Addressable Matrix for Visual-Image Recognition and Behavior Intervention. *Adv. Funct. Mater.* **2018,** *28* (20), 1800275.

(13) Siddiqui, S.; Kim, D.-I.; Roh, E.; Duy, L. T.; Trung, T. Q.; Nguyen, M. T.; Lee, N.-E. A durable and stable piezoelectric nanogenerator with nanocomposite nanofibers embedded in an elastomer under high loading for a self-powered sensor system. *Nano Energy* **2016,** *30*, 434-442.

(14) Yang, R.; Qin, Y.; Dai, L.; Wang, Z. L. Power generation with laterally packaged piezoelectric fine wires. *Nat. Nanotechnol.* **2009,** *4* (1), 34-39.

(15) Zhu, G.; Yang, R.; Wang, S.; Wang, Z. L. Flexible High-Output Nanogenerator Based on Lateral ZnO Nanowire Array. *Nano Lett.* **2010,** *10* (8), 3151-3155.

(16) Hu, Y.; Lin, L.; Zhang, Y.; Wang, Z. L. Replacing a Battery by a Nanogenerator with 20 V Output. *Adv. Mater.* **2012,** *24* (1), 110-114.

(17) Zhu, G.; Wang, A. C.; Liu, Y.; Zhou, Y. S.; Wang, Z. L. Functional Electrical Stimulation by Nanogenerator with 58 V Output Voltage. *Nano Lett.* **2012,** *12* (6), 3086-3090.

(18) Gu, L.; Cui, N.; Cheng, L.; Xu, Q.; Bai, S.; Yuan, M.; Wu, W.; Liu, J.; Zhao, Y.; Ma, F.; Qin, Y.; Wang, Z. L. Flexible Fiber Nanogenerator with 209 V Output Voltage Directly Powers a Light-Emitting Diode. *Nano Lett.* **2013,** *13* (1), 91-94.

(19) Yeo, H. G.; Ma, X.; Rahn, C.; Trolier-McKinstry, S. Efficient Piezoelectric Energy Harvesters Utilizing (001) Textured Bimorph PZT Films on Flexible Metal Foils. *Adv. Funct. Mater.* **2016**, 5940-5946.

(20) Xu, S.; Qin, Y.; Xu, C.; Wei, Y.; Yang, R.; Wang, Z. L. Self-powered nanowire devices. *Nat. Nanotechnol.* **2010,** *5* (5), 366-373.

(21) Wu, W.; Bai, S.; Yuan, M.; Qin, Y.; Wang, Z. L.; Jing, T. Lead Zirconate Titanate Nanowire Textile Nanogenerator for Wearable Energy-Harvesting and Self-Powered Devices. *Acs Nano* **2012,** *6* (7), 6231-6235.

(22) Bai, S.; Xu, Q.; Gu, L.; Ma, F.; Qin, Y.; Wang, Z. L. Single crystalline lead zirconate titanate (PZT) nano/micro-wire based self-powered UV sensor. *Nano Energy* **2012,** *1* (6), 789-795.

(23) Saravanakumar, B.; Thiyagarajan, K.; Alluri, N. R.; SoYoon, S.; Taehyun, K.; Lin, Z.-H.; Kim, S.-J. Fabrication of an eco-friendly composite nanogenerator for self-powered photosensor applications. *Carbon* **2015,** *84*, 56-65.

(24) Bai, S.; Zhang, L.; Xu, Q.; Zheng, Y.; Qin, Y.; Wang, Z. L. Two dimensional woven nanogenerator. *Nano Energy* **2013,** *2* (5), 749-753.

(25) Zhang, L.; Bai, S.; Su, C.; Zheng, Y.; Qin, Y.; Xu, C.; Wang, Z. L. A High-Reliability Kevlar Fiber-ZnO Nanowires Hybrid Nanogenerator and its Application on Self-Powered UV Detection. *Adv. Funct. Mater.* **2015,** *25* (36), 5794-5798.

(26) Han, W.; Zhang, L.; He, H.; Liu, H.; Xing, L.; Xue, X. Self-powered vision electronic-skin basing on piezo-photodetecting Ppy/PVDF pixel-patterned matrix for mimicking vision. *Nanotechnology* **2018,** *29* (25), 255501.

(27) Zhang, L.; Fu, Y.; Xing, L.; Liu, B.; Zhang, Y.; Xue, X. A self-powered flexible vision electronic-skin for image recognition based on a pixel-addressable matrix of piezophototronic ZnO nanowire arrays. *Journal of Materials Chemistry C* **2017,** *5* (24), 6005-6013.

(28) Sinha, T. K.; Ghosh, S. K.; Maiti, R.; Jana, S.; Adhikari, B.; Mandal, D.; Ray, S. K. Graphene-Silver-Induced Self-Polarized PVDF-Based Flexible Plasmonic Nanogenerator Toward the Realization for New Class of Self Powered Optical Sensor. *ACS Appl. Mater. Interfaces* **2016,** *8* (24), 14986-14993.

(29) Khonkar, H.; Alyahya, A.; Aljuwaied, M.; Halawani, M.; Al Saferan, A.; Al-Khaldi, F.; Alhadlaq, F.; Wacaser, B. A. Importance of cleaning concentrated photovoltaic arrays in a desert environment. *Solar Energy* **2014,** *110*, 268-275.

(30) Park, K.-I.; Lee, M.; Liu, Y.; Moon, S.; Hwang, G.-T.; Zhu, G.; Kim, J. E.; Kim, S. O.; Kim, D. K.; Wang, Z. L.; Lee, K. J. Flexible Nanocomposite Generator Made of BaTiO3 Nanoparticles and Graphitic Carbons. *Adv. Mater.* **2012,** *24* (22), 2999-3004.

(31) Xu, Q.; Cheng, L.; Meng, L.; Wang, Z.; Bai, S.; Tian, X.; Jia, X.; Qin, Y. Flexible Self-Powered ZnO Film UV Sensor with a High Response. *ACS Appl. Mater. Interfaces* **2019,** *11* (29), 26127-26133.

(32) Li, Y.; Della Valle, F.; Simonnet, M.; Yamada, I.; Delaunay, J.-J. Competitive surface effects of oxygen and water on UV photoresponse of ZnO nanowires. *Appl. Phys. Lett.* **2009,** *94* (2), 023110.

(33) Wang, Z. L. On Maxwell's displacement current for energy and sensors: the origin of nanogenerators. *Mater. Today* **2017,** *20* (2), 74-82.

(34) Halsall, M. P.; Crowe, I. F.; Mullins, J.; Oliver, R. A.; Kappers, M. J.; Humphreys, C. J. Photomodulated Reflectivity Measurement of Free-Carrier Dynamics in InGaN/GaN Quantum Wells. *ACS Photonics* **2018,** *5* (11), 4437-4446.

(35) Peixian Ye, A. B., Christian Demers, Marguerite-Marie Denariez Roberge, and Xing Wu. Picosecond photoinduced absorption in photorefractive BaTiO3. *Opt. Lett.* **1991,** *16* (13), 980-982.

(36) Zhou, Y.; Liu, W.; Huang, X.; Zhang, A.; Zhang, Y.; Wang, Z. L. Theoretical study on two-dimensional MoS2 piezoelectric nanogenerators. *Nano Res.* **2016,** *9* (3), 800-807.

(37) Xu, Q.; Qin, Y. Theoretical study of enhancing the piezoelectric nanogenerator's output power by optimizing the external force's shape. *APL Mater.* **2017,** *5* (7), 074101.

(38) Xu, Q.; Zhao, Q.; Zhu, X.; Cheng, L.; Bai, S.; Wang, Z.; Meng, L.; Qin, Y. A new kind of transparent and self-cleaning film for solar cells. *Nanoscale* **2016,** *8* (41), 17747-17751.

Table of Contents Graphic

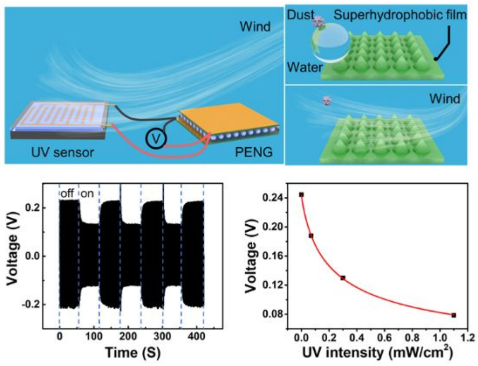

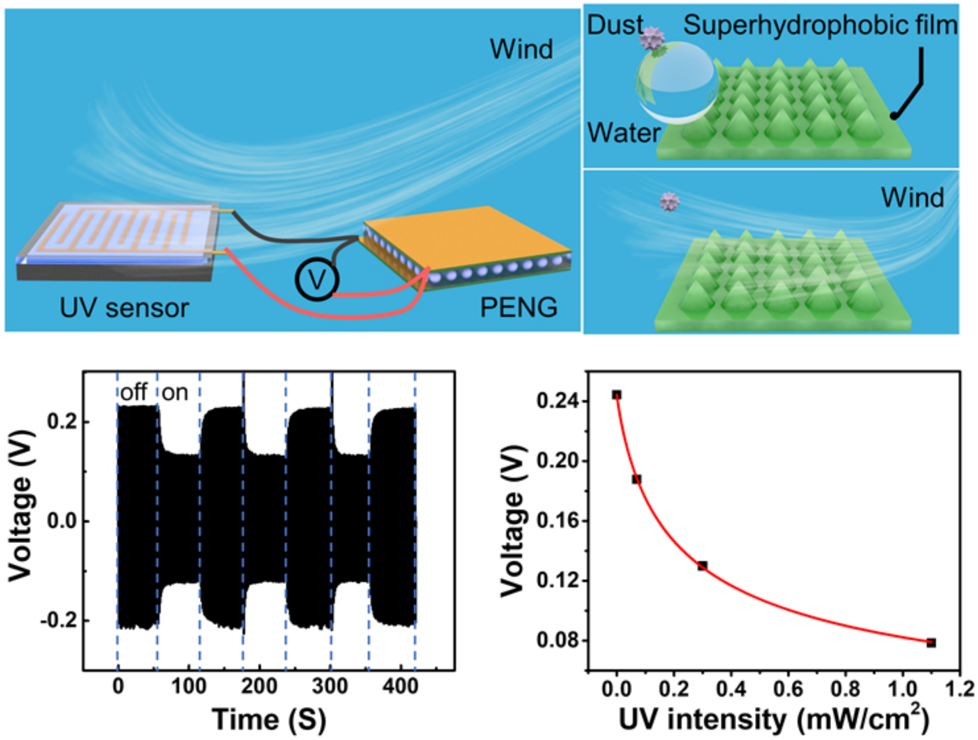

64x47mm (300 x 300 DPI)